ECCOMAS Congress 2016
VII European Congress on Computational Methods in Applied Sciences and Engineering
M. Papadrakakis, V. Papadopoulos, G. Stefanou, V. Plevris (eds.)
Crete Island, Greece, 5–10 June 2016

BLOOD FLOW IN THE COMMON CAROTID ARTERY WITH STENOSIS

Helena A.M. Henriques[1], Luísa C. Sousa[2] , Catarina F. Castro[2], , Carlos C. António[2], Rosa Santos[3], Pedro Castro[3] e Elsa Azevedo[3]

[1]INEGI, Instituto de Ciência e Inovação Em Engenharia Mecânica e Engenharia Industrial
Campus da FEUP, Rua Dr. Roberto Frias, 400, 4200-465 Porto, Portugal
andreina-monteiro@hotmail.com

[2]INEGI and DEMec, Faculdade de Engenharia da Universidade do Porto
Rua Dr. Roberto Frias, s/n, 4200-465 Porto, Portugal
lcsousa@fe.up.pt, ccastro@fe.up.pt, cantonio@fe.up.pt

[3]Departamento de Neurologia, Hospital de S. João e Faculdade de Medicina da Universidade do Porto
Rua Alameda Prof. Hernâni Monteiro, 4200-319 Porto, Portugal
rosampsantos2@gmail.com, pedromacc@gmail.com, elsaazevedo1@gmail.com

Keywords: Ultrasound, Carotid Bifurcation, Segmentation, Hemodynamics.

Abstract. *This work presents the development of a computational methodology based on ultrasound (US) data and able to simulate the hemodynamics of a carotid bifurcation with stenosis. A semi-automatic lumen segmentation methodology of longitudinal and cross-sectional images is presented. The algorithm, implemented in Matlab is based on the hypoecogenic characteristic of the lumen and allows the lumen contour extraction in 2D B-mode images. Patient-specific Womersley velocity profiles, derived from the pulsatile velocity waveforms obtained by pulsed Doppler images, were considered for the definition of the boundary conditions. An image based computational fluid dynamics model of a middle-aged patient was reconstructed from both segmented transversal and longitudinal US images. The blood flow simulation was performed using the Ansys/Fluent software. Pulsatile conditions of the hemodynamic analysis were validated by the carotid US scan. Hemodynamic analysis was performed based on wall shear stress (WSS) descriptors. High values of time-averaged wall shear stress (TAWSS) were captured within stenosis. Low values of TAWSS where found at the carotid bulb, upstream and downstream stenosis and also at external carotid artery. In these regions the oscillatory shear index (OSI) and the relative residence time (RRT) present high values, in agreement with the fact these hemodynamic descriptors are able to capture abnormal flow conditions witch present an import role in the local development of atherosclerotic plaques. This study shows to be clinically useful in the diagnosis and management of the treatment of carotid stenosis as it is able to show a complex hemodynamic behaviour during the cardiac cycle allowing the correlation between the carotid wall pathophysiology and the local influence in artery hemodynamics.*

1 INTRODUCTION

Atherosclerosis is a degenerative disease of the arteries resulting in plaques that can cause stenosis, embolization and thrombosis. In the past decades, several studies based on computational fluid dynamics (CFD) showed that hemodynamic factors are associated with the development and progression of the disease, determining the local distribution of plaques [1-4] However, as hemodynamic phenomena is not yet fully understood, detailed study of disturbed flow during the cardiac cycle may give additional insight to understanding the progression of atherosclerosis being useful in clinical diagnosis.

Due to the anatomy of the head neck region, the use of sonography for diagnostic is integrated in daily clinical routine; it is a fast and inexpensive technique, extremely useful in the initial evaluation of symptomatic patients and enables the acquisition of the carotid artery bifurcation geometry. Automatic segmentation of US images is a complex work due to poor imaging quality as low contrast, speckle, echo shadows and artifacts. Segmentation methods based on active contours, and parametric snakes are not the best choice for an automatic and accurate segmentation of the carotid artery wall; they are based on intensity gradients and require manual initialization, with the design of the initial contour [5, 6].

Previous works on patient-specific hemodynamic combining manual or semi-automatic image segmentation with finite element blood flow simulation have been performed [7, 8]. Like those studies this research presents a patient-specific study, considering a three-dimensional (3D) model of the bifurcation wall reconstructed from segmented B-mode US and blood flow velocity spectral waveforms obtained from PW Doppler images. Carotid artery bifurcation reconstruction based on a set of segmented longitudinal and transversal US images was considered as input geometry of the 3D model for computational fluid dynamics. The assumptions of an incompressible and Newtonian fluid, rigid vascular wall and non-slip condition were considered. Pulsatile inlet boundary conditions obtained from Doppler US measurements are applied at the entrance of the common carotid artery (CCA). This study presents a new segmentation methodology based on pixel intensity distribution and region growing and hemodynamic simulation is performed using ANSYS Fluent 14.5 package.

2 METHODS

The patient-specific hemodynamic study presented is done using Doppler US imaging data; five sequential steps are required [7, 8]: data acquisition, lumen segmentation of longitudinal and transversal carotid images, 3D carotid bifurcation surface reconstruction, mesh generation and hemodynamic simulation.

Data was obtained at São João Hospital Centre, a university hospital in Porto, Portugal. Carotid artery examinations were performed according to a proposed created protocol; this study was approved by the institutional ethical committee and informed consent of each volunteer was obtained.

2.1 Data aquisition

Experimental data necessary for the present study were obtained by the same experienced sonographer (R.S.) dedicated to neurovascular ultrasound at the Neurosonology Unit of the Department of Neurology of São João Hospital Centre [7, 8].

For a middle aged patient of 57 years old man with a high grade stenosis, B-mode and pulsed-wave (PW) Doppler images were collected along the CCA, its bifurcation and proximal segments of internal carotid artery (ICA) and external carotid artery (ECA) including the bifurcation entrance (APEX). For this purpose a commercial colour US scanner (Vivid e; GE, Milwaukee, WI, USA) and a linear array probe (GE 8L-RS) were used. The longitudinal and

transversal set of B-mode images was recorded at end-diastole, to control physiologic variations of diameter within cardiac cycle. Cross-sectional locations were registered at the longitudinal bifurcation image, to allow the correct reconstruction of the CCA bifurcation luminal surface. In order to minimize flow modelling inaccuracies, tracking of the US probe was done by marking positions along the artery bifurcation relying on the ability to manually guide the US probe. During medical examination, ICA stenosis was measured according to European Carotid Surgery Trial (ECST), the percentage of luminal diameter narrowing at the most stenotic region.

Using US PW mode with a 2 mm sample volume, axial flow velocity waveforms were obtained at several specific locations along CCA and distal region of ICA and ECA arteries that could be measured with angle of insonation $\leq 60^{o}$. Considering waveform data from three cardiac cycles Fourier analysis allowed the determination of the first seven harmonics coefficients used to set Womersley profiles.

2.2 Imaging segmentation and carotid bifurcation geometry definition

Segmentation of acquired B-mode images is a complex work due to poor imaging quality as low contrast, speckle, echo shadows and artifacts. Segmentation of the transversal images is more difficult because contour lumen is discontinuous as they present more artifacts caused by speckle noise. A semi-automatic algorithm was implemented using MATLAB software. After converting the colour image to gray levels the selection of the four corners delimiting the rectangular region of interest is performed and the region of interest is selected as shown in figure 1a).

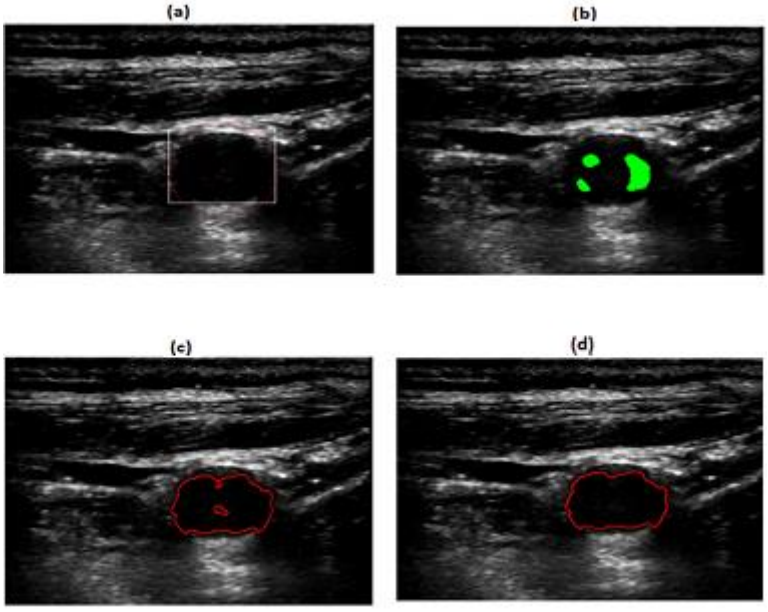

Figure 1: Transversal CCA lumen segmentation: (a) Selection of the region of interest and increased overall image contrast; (b) Identification of lumen central region; (c); (d) Lumen segmentation by region growing.

The identification of the lumen central region is made applying the histogram equalization (CLAHE) and a Gaussian filter smoothing. To identify the central lumen, the seed points for the lumen segmentation algorithm, the method proposed by Molinari et al. (2007) [9], was followed; like in this method, carotid features in an image are addressed as a distribution model of variable intensity along the carotid regions and 2D histograms for mean and stand-

ard deviation were calculated for the establishment of lumen selection criteria. The identified lumen central region is presented in figure 1b).

Region growing segmentation methods are based on grouping sets of neighbouring pixels that meet defined similarity criteria, figures 1c) and 1d). For this study, the considered similarity criterion was taken as the average intensity of a neighbourhood window of 10 × 10 pixels after applying the DSFSRAD filter. An iterative process consisting in checking every pixel just outside the border of the lumen central region was performed; if the homogeneity criterion is validated (intensity is smaller than 0.027) the new pixels will join the newly enlarged lumen central region. The iterative process finishes when enlargement of the region becomes impossible.

After imaging segmentation, 2D smooth lumen contours were stacked in the axial direction according to each image location obtained during data acquisition. The reconstructed lumen surface was smoothed in order to reduce misalignment errors due to patient's involuntary movements during scan.

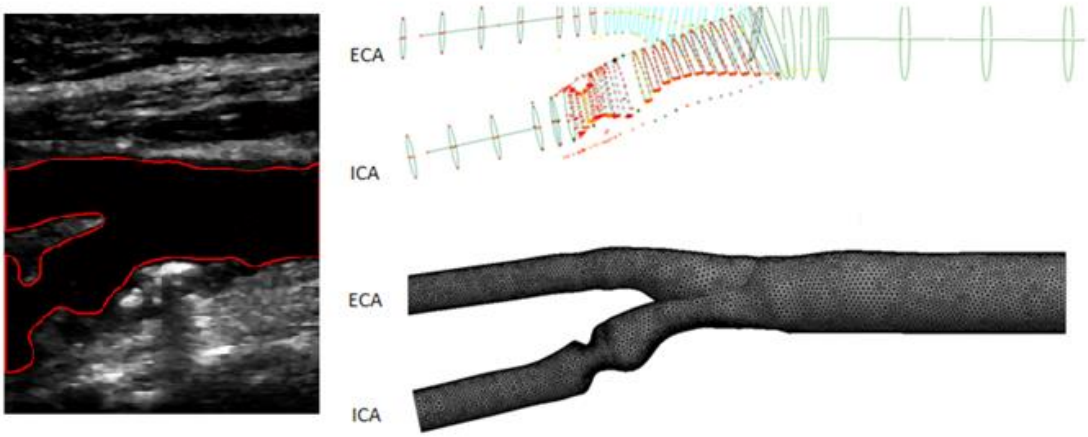

Figure 2: 3D model: segmented longitudinal image, wall surface reconstruction and fluid volume mesh.

The obtained carotid bifurcation surface was not directly usable for generating a suitable computational mesh. Cylindrical flow extensions with a length of four times the local diameters were added at the inlet (before bifurcation) and outlet (after bifurcation) locations, in the direction of the centreline, in order to ensure fully developed velocity profiles at the inlet and to minimize the influence of outlet boundary conditions.

2.3 Meshing and blood flow simulation

Tetrahedral mesh was generated using the software Ansys Workbench (figure 2). The quality of the mesh was tested under steady-state conditions. Using meshes with increasing resolution, the adopted mesh was chosen when a relative error of nodal WSS lower than 5% was reached.

Commercial package Ansys Fluent 14.5 was used to simulate pulsatile blood flow. The first order implicit backward Euler method was considered for the temporal discretization of the Navier-Stokes equations and converged solutions searched using the SIMPLE algorithm and the second-order upwind scheme with a maximum of 40 iterations for each time step. Blood was modelled as a viscous Newtonian fluid [4], incompressible and isotropic with a density of 1060 kg/m3 and a dynamic viscosity of 0.0035 kg/(m.s). At the entrance of the CCA, Womersley velocity profiles derived from pulsatile velocity waveforms extracted from patient PW Doppler images were imposed [7, 8]; a zero wall motion was assumed as in dis-

eased vessels wall motion is further reduced. Outflow boundary conditions were imposed considering a constant flow ratio ICA/ECA = 70%/30%. Three cardiac cycles were simulated considering a constant time step equal to 0.008 seconds. The flow velocities and the WSS vectors from the last cycle were recorded for post-processing.

3 RESULTS AND DISCUSSION

The distribution of velocities at systolic peak is shown in Figure 3. As expected, high velocities were detected at ICA stenosis. Stagnation zones and high velocity gradients can be noticed near the outer bulb wall, opposite to the bifurcation divider wall and downstream stenosis, due to the high variability of the lumen arterial sectional area.

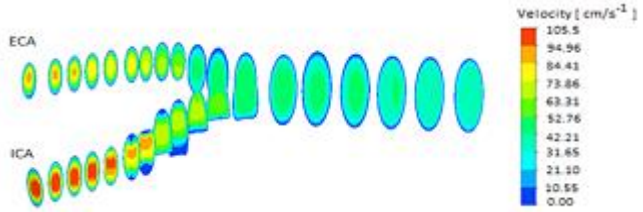

Figure 3: Velocity field at systolic peak (top).

In this work the most widely used WSS-based descriptors, the time-averaged WSS (TAWSS), the oscillating shear index (OSI) and the relative residence time (RRT) were adopted to measure low and oscillating shear stress at the carotid bifurcation [10].

Figure 4 presents the distribution of the wall shear stress based descriptors, shown on the anterior and posterior side of the carotid artery. Low values of TAWSS can be found at ICA origin and upstream and downstream stenosis identifying flow disturbances. Low TAWSS values appeared also on the distal inner wall of ECA. TAWSS values, lower than 0.4 Pa, are associated with intima/media thickening and moderate TAWSS values, larger than 1.5 Pa, induce quiescence and atheroprotective gene expression profile.

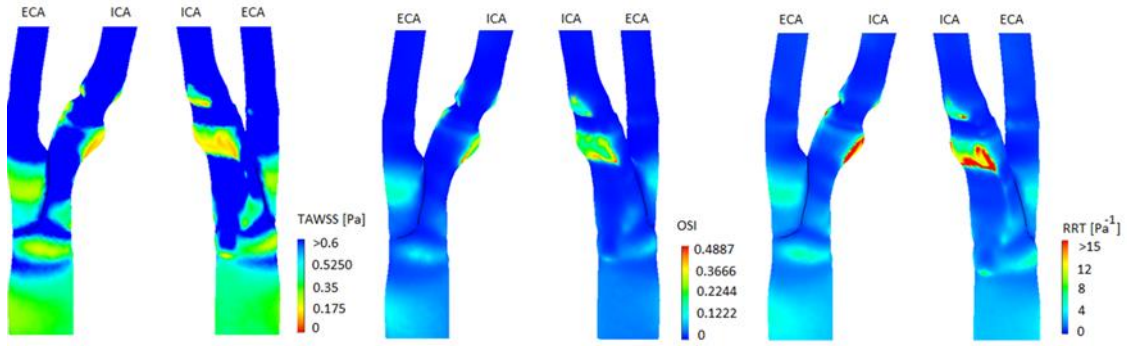

Figure 4: Wall shear stress descriptors: TAWSS (left), OSI (center) and the RRT (right).

In figure 4, OSI and RRT high values regions coincide with TAWSS low values sites; all the hemodynamic indexes captured apparent abnormal flow disturbances at the same sites, ICA origin, upstream and downstream stenosis and in distal inner wall of ECA. Previous studies identify the same regions corresponding to recirculation zones, areas of greater turbulence, and consequently a high shear oscillation [2, 3, 11]. In this work WSS-based descriptors show to be correlated as sites of extremes for TAWSS coincide with sites of extremes of the two other descriptors. Some authors recommended the RRT as a robust single metric of low and oscillatory shear stress [2-4].

4 CONCLUSIONS

This study combined computational 3D geometry reconstruction and simulation of blood flow characteristics in a carotid artery bifurcation based on Doppler images. Using patient-specific carotid artery US data collected in hospital practice, a semi-automatic reconstruction of a carotid bifurcation geometry was presented in this work. A new semiautomatic segmentation algorithm for the lumen contour extraction in US longitudinal 2D B-mode images was presented. This semiautomatic algorithm is robust with respect to factors that degrade this type of images, including appearance of artifacts, lots of speckle noise and occlusions of the lumen caused by plaque region. The algorithm provides a good estimate of the lumen contour when compared with a manual contour and showed to be able to segment the carotid lumen of a stenosed bifurcation.

The simulation demonstrated several complex flow features near the stenosis associated with the diseased vessel geometry. All WSS-based descriptors, assigned highly disturbed flows at the same artery surface regions, as they were able to capture abnormal flow at carina and upstream and downstream ICA stenosis.

Further research will be needed to understand the effect of wall compliance on the blood flow patterns of specific severely diseased carotid arteries. In order to elucidate the role of carotid hemodynamics on plaque development and plaque vulnerability, further larger studies should be done, providing clinically relevant information for risk assessment and surgical planning.

5 ACKNOWLEDGEMENTS

The authors gratefully acknowledge the funding by FCT, Portugal, of the Research Unit of LAETA-INEGI, Faculdade de Engenharia da Universidade do Porto.

REFERENCES

[1] G. De Santis, M.Conti, B. Trachet, T. De Schryver, M. De Beule, J. Degroote, J. Vierendeels, F. Auricchio, P.Segers, P. Verdonck, B. Verhegghe, Haemodynamic impact of stent-vessel (mal)apposition following carotid artery stenting: mind the gaps! *Computer Methods Biomech Biomed Engin*, **16**(6), 648-59, 2013.

[2] S. Lee, L. Antiga, D. Steinman, Correlations among indicators of disturbed flow at the normal carotid bifurcation. *Journal of Biomechanics Engineering*, **131**(6), 061013, 2009.

[3] U. Morbiducci , D. Gallo, D. Massai, F. Consolo, R. Ponzini, L. Antiga, C. Bignardi, M.A. Deriu, A. Redaelli, Outflow conditions for image-based hemodynamic models of the carotid bifurcation: implication for indicators of abnormal flow. *Journal of Biomechanics Engineering,* **132**(9), 091005, 2010.

[4] U. Morbiducci , D. Gallo, D. Massai, R. Ponzini, H.A. Deriu, L. Antiga, L. Redaelli, F. Montevecchi, On the importance of blood rheology for bulk flow in hemodynamic models of the carotid bifurcation. *Journal of Biomechanics,* **44**(13), 2427–2438, 2011.

[5] C.P. Loizou, C. Theofanous, M. Pantziaris, T. Kasparis, Despeckle filtering software toolbox for ultrasound imaging of the common carotid artery. *Computer Methods and Programs in Biomedicine,* **114**(1), 109-24, 2014.

[6] Z. Ma, R.N. Jorge, T. Mascarenhas, J.M.R.S. Tavares, A Review of Algorithms for Medical Image Segmentation and their Applications to the Female Pelvic Cavity. *Computer Methods in Biomechanics and Biomedical Engineering*, **13**, 235–246, 2010.

[7] L.C. Sousa, C.F. Castro, C.C. António, A. Santos, R. Santos, P. Castro, E. Azevedo, J.M.R.S. Tavares, Towards hemodynamic diagnosis of carotid artery stenosis based on ultrasound image data and computational modelling. *Medical & Biologcal Engineering & Computing*, **52**(11), 971-83, 2014.

[8] L.C. Sousa, C.F. Castro, C.C. António, F. Sousa, R. Santos, P. Castro, E. Azevedo, Computational simulation of carotid stenosis and flow dynamics based on patient ultrasound data - A new tool for risk assessment and surgical planning. *Advances in Medical Sciences*, **61** (1), 32–39, 2016.

[9] F. Molinari, W. Liboni, E. Pavanelli, P. Giustetto, S. Badalamenti, J.S. Suri, Accurate and automatic carotid plaque characterization in contrast enhanced 2D ultrasound images. Conf. Proc. IEEE Eng. Med. Biol. Soc. 335–338 (2007)

[10] D. Ku, D. Giddens, C. Zarins, S. Glagov, Pulsatile flow and atherosclerosis in the human carotid bifurcation—positive correlation between plaque location and low and oscillating shear-stress. *Arteriosclerosis*, **5**(3), 293–302, 1985.

[11] Y.P. Lian, Y. Liu, X. Zhang, Coupling of membrane element with material point method for fluid–membrane interaction problems. *International Journal Mechanics and Materials in Design.***10** (2), 199–211, 2014.